Journal of Nuclear Materials 390–391 (2009) 822–825

Contents lists available at ScienceDirect

Journal of Nuclear Materials

journal homepage: www.elsevier.com/locate/jnucmat

Experimental verification of FOREV-2D simulations for the plasma shield

S. Pestchanyi *, I. Landman

Forschungszentrum Karlsruhe, IHM, P.B. 3640, D-76021 Karlsruhe, Germany

ARTICLE INFO

PACS:
52.40.Hf
52.55.Fa
52.30.Ex

ABSTRACT

Analysis of experiments in the MK-200UG facility dedicated to verify the FOREV-2D simulations of ITER core contamination with carbon vaporized during ELMs has been performed. In these experiments the carbon fibre composite (CFC) of NB31 grade have been treated with plasma heat fluxes relevant for ITER ELMs. The analysis revealed that thin layer of few hundred microns on CFC surface is damaged and its thermoconductivity effectively reduced approximately three times, but the CFC bulk has the reference thermoconductivity. Good agreement between the measured and the calculated profiles for carbon plasma electron density at various hydrogen plasma heat loads as well as the agreement between the measured and the simulated dependences of the absorbed energy density on the applied heat load provide reliable validation of the carbon plasma shields simulated with the FOREV-2D code. High carbon plasma shield densities of 10^{23}–10^{24} m^{-3} predicted in the simulations for ELM-produced shields has been proved in these MK-200UG experiments.

1. Introduction

ELMy H-mode is the reference operational scenario for the experimental tokamak reactor ITER because of its thermonuclear gain much higher compared with the L-mode. However, the edge localized modes (ELM) of plasma instabilities, intrinsic for this regime, provide short periodic outbursts of heat flux at the carbon fibre composite (CFC) divertor armour of 2–3 orders of the magnitude over its background value. The type I ELMs in ITER would result in the divertor armour vaporization. Vaporized carbon plasma can contaminate the thermonuclear plasma in the ITER core decreasing plasma temperature and the fusion gain or even run the confinement into the disruption. Calculations of the carbon amount vaporized during type I ELMs of sizes typical for ITER have been done earlier [1] using the FOREV-2D code [2–5]. According to these estimates the total number of vaporized carbon atoms varies more than one order of the magnitude, between 6×10^{21} and 2×10^{23} atoms per ELM, increasing with the ELM size. Under the action of thermonuclear plasma released in ELM the carbon is ionized immediately after its vaporization and, the carbon plasma is transported along the magnetic field lines to SOL thus contaminating the ITER core. According to the FOREV simulations the vaporized carbon plasma shield density close to the divertor armour reaches 10^{23}–10^{24} m^{-3} and the carbon plasma is transported to the SOL during 1–3 ms with the characteristic density 10^{20}–10^{21} m^{-3} there. The carbon plasma shields the armour from further heating before the end of the ELM and stops its vaporization. For large type I ELMs the divertor armour shielding plays major role in plasma–wall interaction. The simulations revealed that the plasma shielding efficiency is not constant; it grows with the ELM size decreasing the heat flux by more than one order of the magnitude for very powerful ELMs.

Among the modern tokamaks the type I ELMs with the divertor target heat load $Q > 0.7$ MJ/m^2, enough for the divertor armour vaporization are possible in JET only, but the contamination plasma parameters measurements are still not done there. However, test for simulation of the shielding efficiency done with FOREV-2D code is possible in the MK-200UG plasma gun facility with plasma parameters closest possible for the thermonuclear plasma during ITER ELMs.

This paper describes verification of the plasma shield parameters simulated with FOREV-2D code, which is done using dedicated experiments in MK-200UG facility. Measurements of the absorbed energy dependence on the applied energy have been done as well as corresponding carbon plasma shield densities and temperatures. The measured parameters are compared with the simulated ones confirming the FOREV-2D estimations on carbon contamination of the ITER core after ELMs. Plasma shielding reduces the heat flux to the solid CFC armour if the surface temperature exceeds the vaporization temperature T_{vap}. Vaporized and ionized carbon protects the heated surface from further heating. For the surface heating with different heat fluxes, but with equal time duration τ one can define the maximum value Q_{max} for energy absorbed by the armour. One can explain the existence of Q_{max} without going into details of heating and shielding. It corresponds for the energy conducted inside the solid armour during the time τ if the surface

* Corresponding author. Address: Hermann-von-Helmholtz-Platz 1, Eggenstein-Leopoldshafen, Germany.
E-mail address: sergey.pestchanyi@ihm.fzk.de (S. Pestchanyi).

0022-3115/$ - see front matter © 2009 Elsevier B.V. All rights reserved.
doi:10.1016/j.jnucmat.2009.01.217

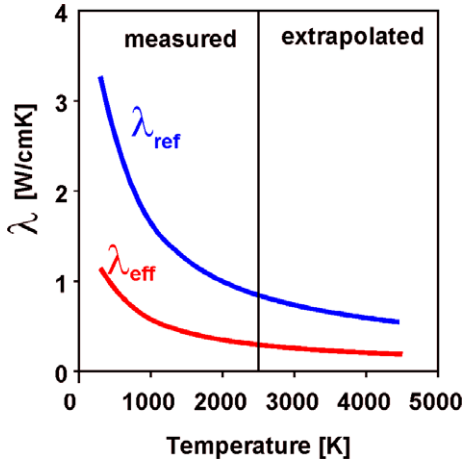

Fig. 1. Reference thermoconductivity for the rectangular NB31 CFC sample in directions of pitch fibres and the effective dependence $\lambda_{eff}(T) = 0.35\lambda_{ref}(T)$ which fits experiments in MK200UG.

temperature maintained equal to the maximal possible value – T_{vap} during heating time τ. Therefore Q_{max} depends on the armour thermoconductivity, vaporization temperature and heating time τ only, but does not depend on the heat flux due to the flux dissipation in the plasma shield. The shielding can be as strong as needed, so for very high heat fluxes, exceeding the value $q = Q_{max}/\tau$ several times the absorbed energy cannot be larger than Q_{max}. However, the plasma shield density grows with the heating flux. In ITER the plasma produced from the divertor armour during ELM, transported in the SOL and thus will contaminate the core. So, the amount of carbon plasma produced by ELMs for the shielding defines the core contamination and hence the thermonuclear gain of the reaction or even the discharge stability.

2. Estimation of NB31 thermoconductivity from experiments in MK-200UG

For investigation of plasma shielding effect a series of the dedicated experiments have been performed in the MK-200UG facility and the results are reported in [6]. First analysis of the surface temperature measurements of the NB31 target in the MK-200UG facility have been performed and revealed that the measurements are definitely incompatible with the reference thermoconductivity of NB31 CFC [7,8] shown in Fig. 1. However, all the measurements are matching with the simulations if one assumes the effective thermoconductivity approximately three times lower

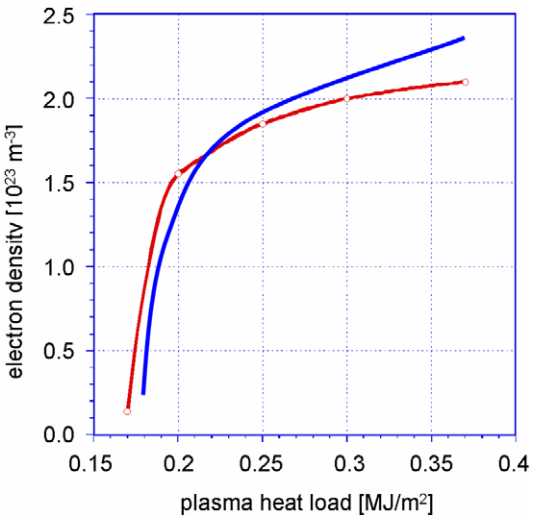

Fig. 3. Electron density of carbon plasma versus plasma heat load (1 cm from CFC target surface, 10–15 μs after start of plasma/target interaction). Shown are the curve (with circles) measured in the MK-200UG facility and the results of FOREV-2D simulations with $\lambda_{eff}(T) = 0.35\lambda_{ref}(T)$.

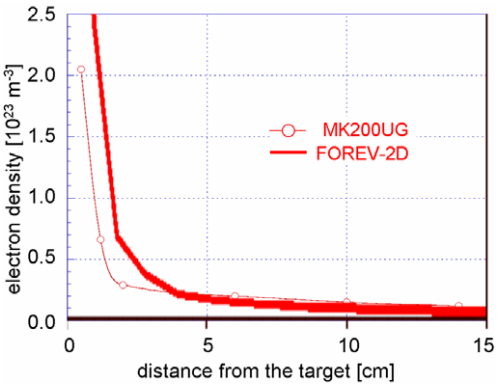

Fig. 4. Comparison of the measured and simulated space distribution of electron density in front of the CFC target for the plasma shot in MK-200UG with the heat load of 0.3 MJ/m^2, at 13 μs after start of plasma–wall interaction, $\lambda_{eff}(T) = 0.35\lambda_{ref}(T)$.

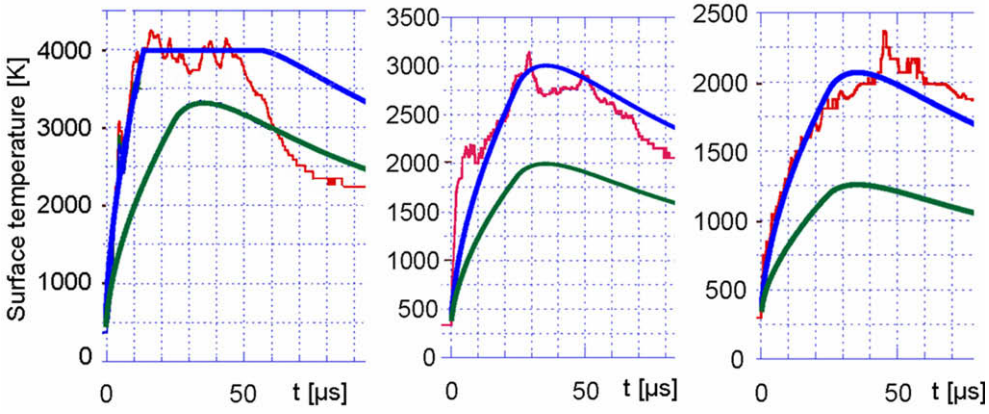

Fig. 2. Comparison of the measured and numerically simulated time dependences of the surface temperature for three shots in the MK-200UG facility. The plasma heat loads are 0.24 MJ/m^2, 0.145 MJ/m^2 and 0.09 MJ/m^2 from left to right. Two numerical curves (smooth) for each shot correspond to simulations with the reference thermoconductivity (lower curve) and for the thermoconductivity reduced by factor 0.35 (upper curve).

than the reference value at all the temperatures $\lambda_{eff}(T) = 0.35\lambda_{ref}(T)$ [6]. Further simulations of these experimental results using the FOREV-2D code confirmed this conclusion. Generally speaking the discrepancy between the measured and simulated dependences for surface temperature can be explained, for example, assuming that $\lambda(T)$ drops at $T > 2500$ K where the thermoconductivity is unknown and the analytical approximation is used for the simulations. However, comparison of the measured and numerically simulated time dependences of the surface temperature for three shots with plasma heat loads of 0.24 MJ/m^2, 0.145 MJ/m^2 and 0.09 MJ/m^2 in the MK-200UG facility shown in Fig. 2 allows rejecting this possibility. The time dependence is fitted at lower temperatures, especially for the shot with 0.09 MJ/m^2 heat load. For this shot temperature was always in the range of the directly measured thermoconductivity.

Additional arguments for the thermal conductivity degradation of CFC under repeated thermoshocks have been deduced from the experiment with plasma shield density measurements performed at the same MK-200UG facility. A series of dedicated experiments has revealed that vaporization from the heated CFC surface starts at total energy load of 0.17 MJ/m^2 providing the carbon plasma density of $2–3 \times 10^{22}$ m^{-3} at the distance of few millimetres above the surface [6]. At the heat load of 0.2 MJ/m^2 the vapour density close to the surface increases 10 times and remains almost unchanged due to shielding of the surface from the hot hydrogen plasma. Calculation of the NB31 vaporization threshold in the MK-200UG facility has shown that with the reference thermoconductivity it should start at 0.3 MJ/m^2 – the value, which is far beyond the accuracy of the measurements. But, the same reduction coefficient, which was used for fit of the temperature measurements, gives rise to the sublimation threshold value of 0.17 MJ/m^2 measured in this set of experiments in MK-200UG.

However, surface temperatures measured during stationary mock-up heating [9] are in a reasonable agreement with the reference CFC thermoconductivity $\lambda_{ref}(T)$. This discrepancy is resolved assuming that only a thin surface layer of few hundred microns is damaged and the CFC bulk has the reference thermoconductivity. If so, in stationary heating regime the temperature drop inside the damaged layer with reduced thermoconductivity is small comparing with the total temperature difference across the mock-up of ~1 cm thickness. But for fast heating with the characteristic time less then 100 μs, like in the MK200UG facility only the damaged layer with $\lambda_{eff}(T) = 0.35\lambda_{ref}(T)$ is involved and the thermoconductivity of the CFC bulk plays no role. The reason for the thermoconductivity degradation (described in [10]) is the large number of cracks developed in the layer of 100–200 μm thickness at the CFC surface in course of several hundred severe thermal shocks, performed before the surface temperature measurements for simulation of the ELM-like heat loads.

3. Plasma shield in MK-200UG and its FOREV-2D simulations

FOREV-2D has been updated to simulate the MK-200UG plasma stream of ~50 μs time duration with the maximum electron temperature of 200 eV, the maximum energy of hydrogen ions of 2 keV at the stream axis and the density of the plasma varying to simulate different plasma loads. The plasma in MK-200UG facility fully magnetized in 2 T field. Comparison of the measured and simulated plasma shield densities at 1 cm distance from CFC target surface at 10–15 μs after start of plasma/target interaction is shown in Fig. 3. The experimentally measured curve is in a reasonable agreement with the simulation performed using FOREV-2D code with the thermoconductivity reduced by the same factor 0.35 as for the surface temperature simulations. Further comparison of space distribution for the electron density in front of the target available from measurements in MK-200UG facility with the simulations illustrated in Fig. 4 shows the good agreement too. Shown is the space distribution of the electron density at 13 μs after start of plasma–wall interaction for plasma heat load of 0.3 MJ/m^2.

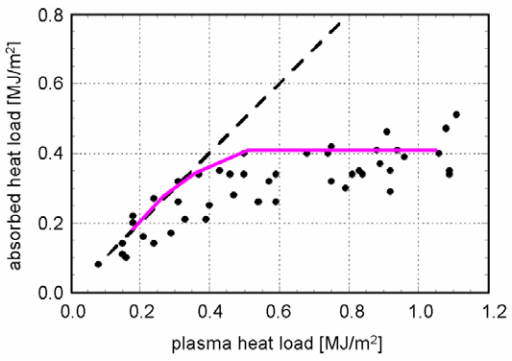

Fig. 5. Comparison of the measured and simulated dependences of the energy absorbed by the CFC target from the plasma load. The simulated curve corresponds to the CFC target consisting of 28% of pitch fibres and 72% of the matrix and PAN fibres with $\lambda_{eff}(T) = 0.35\lambda_{ref}(T)$.

The dependence of the energy absorbed by the target on the applied energy has been measured in the MK-200UG facility and reported in [6]. Simulations of these measurements have been performed using the FOREV-2D code. Comparison of the measured and simulated dependences is shown in Fig. 5. NB31 CFC consists of 28% of pitch fibres, perpendicular to the irradiated CFC surface in addition to 72% of the PAN fibres and matrix. Results of the FOREV-2D simulations have shown that the energy density absorbed by the CFC matrix and PAN fibres saturates at the level of $Q_{abs} = 0.26$ MJ/m^2 and the absorbed energy density for the pitch fibres saturates at the level of $Q_{abs} \sim 1.0$ MJ/m^2, assuming that the pitch fibres thermoconductivity degraded in the same way as the PAN fibres and the matrix: $\lambda_{eff}(T) = 0.35\lambda_{ref}(T)$. Supposing approximately 1D heat transport inside the CFC target one can combine the above calculated values to obtain the saturation $Q_{abs} \sim 0.34$ MJ/m^2, which is reasonably close to the measured value and definitely inside the error bar of the experimental data. The resulting curve for the absorbed energy dependence is plotted in Fig. 5 together with the measured points.

4. Conclusions

Two series of experiments have been performed in the MK-200UG facility for verification of FOREV-2D simulations of ITER core contamination with carbon vaporized during ELM [1]. In these experiments the CFC NB31 targets have been treated with plasma heat fluxes relevant for ITER ELMs. The targets were exposed to hot magnetized hydrogen plasma streams at heat loads of $Q = 0.05–1$ MJ/m^2 and the pulse duration of $\tau = 0.05$ ms. CFC vaporization and properties of the vaporized carbon plasma have been studied experimentally and analyzed numerically.

The numerical simulations of the CFC vaporization, evolution of the CFC surface temperature and the plasma shield parameters have revealed that the measurements are definitely incompatible with the reference thermoconductivity of NB31. However, all the measurements agree with the simulations if the effective thermoconductivity is assumed to be approximately three times lower than the reference value $\lambda_{eff}(T) = 0.35\lambda_{ref}(T)$. Degradation of the thermoconductivity was caused by brittle destruction during multiple plasma exposures simulating the ELM-like heat loads and performed before the measurements. Using $\lambda_{eff}(T) = 0.35\lambda_{ref}(T)$ in the FOREV-2D calculations one can successfully match all the measured electron density, and surface temperature profiles and the threshold value for the CFC vaporization start.

The measured dependence of the absorbed energy density on the incident plasma heat loads for the matrix and the PAN fibres differs considerably from the simulated data, even with the thermoconductivity reduced by the factor 0.35. Taking into account the heat absorbed by the pitch fibres restores the agreement. However, all these measurements are in contradiction with the measurements of NB31 CFC loading with stationary heat flux. The surface temperatures measured during stationary mock-up heating are in a reasonable agreement with the reference CFC thermoconductivity $\lambda_{ref}(T)$. This contradiction is resolved assuming that only a thin surface layer of few hundred microns is damaged and the CFC bulk has the reference thermoconductivity. So, for stationary heating the thermoconductivity $\lambda_{eff}(T) = \lambda_{ref}(T)$, but for fast heating characteristic for ITER ELMs $\lambda_{eff}(T) = 0.35\lambda_{ref}(T)$.

Good agreement between the measured and the calculated carbon plasma electron density profiles at various hydrogen plasma heat loads and the absorbed energy density dependence on the incident heat load provide a reliable validation of the results of the FOREV-2D code simulations for the cold carbon plasma production during ITER ELMs. High carbon plasma shield densities of 10^{23}–10^{24} m^{-3} predicted in the simulations of ELMs has been proved in the MK-200UG experiments.

Acknowledgements

This work, supported by the European Communities under the contract of Association between EURATOM and Forschungszentrum Karlsruhe, was carried out within the framework of the European Fusion Development Agreement. The views and opinions expressed herein do not necessarily reflect those of the European Commission.

Authors gratefully acknowledge Dr V.M. Safronov, for providing the results of the experiments on MK-200UG facility and Dr J. Linke for the information on divertor mock-up experiments in the JUDITH facility and for the fruitful discussions during analysis of their results.

References

[1] S. Pestchanyi, I. Landman, J. Nucl. Mater. 363–365 (2007) 1081.
[2] H. Wuerz, S. Pestchanyi, F. Kappler, Fus. Eng. Des. 49&50 (2000) 389.
[3] H. Wuerz, S. Pestchanyi, F. Kappler, et al., Hot Plasma Target Interaction and Quantification of Erosion of the ITER Slot Divertor During Disruptions and ELMs, Forschungszentrum Karlsruhe, Wissenschaftliche Berirchte FZKA 6198, March 1999.
[4] S.E. Pestchanyi, I.S. Landman, Implementation of Tokamak Magnetic Flux Coordinates and Divertor Geometry in Disruption/ELM Simulation Code FOREV-2, EFDA, Technology Work ProgramTW3-TPP-DISELM, Final Report December 2003.
[5] S.E. Pestchanyi, I.S. Landman, H. Wuerz, Hot plasma contamination in ELMs by divertor material, in: Proceedings of 30th EPS Conference on Controlled Fusion and Plasma Physics, St. Petersburg, Russia, 2003.
[6] V.M. Safronov, N.I. Arkhipov, I.S. Landman, S.E. Pestchanyi, D.A. Toporkov, A.M. Zhitlukhin, J. Nucl. Mater., in press (ICFRM-13 Nice, 10–15 December 2007).
[7] J.P. Bonal, D. Moulinier, Thermal Properties of Advanced Carbon Fiber Composites for Fusion Application, Rapport DMT/95-495, CEA, Direction des reacteurs nucleaires, Depertement de mecanique et de technologique, October 1995.
[8] I. Berdoyes, Snecma Propulsion Solide, Technical Note, Reference FPTM0393200A, 12 October 2003.
[9] M. Roedig, R. Duwe, K. Kuehnlein, J. Linke, M. Scheerer, I. Smid, B. Wiechers, J. Nucl. Mater. 258–263 (1998) 967.
[10] S.E. Pestchanyi, I.S. Landman, Phys. Scr. T111 (2004) 218.